

## Deep Fluorescence Solvatochromic Study of Nitrogen Doped Carbon Dots: Polar Sensitive Nanoprobe Application

M. Kaviani Darani<sup>1</sup>, Sh. Rouhani<sup>\*1</sup>, Z. Ranjbar<sup>2</sup>

1. Department of Organic Colorant, Institute for Color Science and Technology, P. O. Box: 16765-654, Tehran, Iran.

2. Department of Surface Coatings and Corrosion, Institute for Color Science and Technology, P.O. Box: 16765-654, Tehran, Iran

### ARTICLE INFO

Article history:

Received: 7 Sept 2024

Final Revised: 17 Dec 2024

Accepted: 21 Dec 2024

Available online: 08 Mar 2025

Keywords:

Solvatochromic

Nitrogen doped

Carbon dots

Phenylenediamine

Binary solvent

Humidity sensing

### ABSTRACT

**I**n this research, we synthesized nitrogen-doped carbon dots using three isomers of phenylenediamine (*o*-PDA, *m*-PDA, and *p*-PDA) as nitrogen sources and citric acid as the carbon source. We selected these isomers to study their effect on surface chemistry and optical characteristics. The carbon dots produced contain nitrogen, carboxyl, and hydroxyl groups that interact with the environment and exhibit a change in emission based on the surroundings. Our team conducted an in-depth analysis of the fluorescence emissions exhibited by carbon dots. The study involved examining the behavior of these particles in solvents with varying degrees of polarity, ranging from weakly polar  $CHCl_3$  to strongly polar protic water and a binary mixture of  $H_2O$ -Acetone. The results of the study provide valuable insights that could contribute to advancing our understanding of carbon dots properties. Interestingly, with increasing the water content of organic solvents, the carbon dots changed their fluorescence color from blue to green. We utilized the Lippert-Mataga plot to exhibit a direct correlation between polarity and carbon dots emission wavelength, which demonstrated a positive linear trend as the polarity was increased. The slope for the three isomers was  $\Delta\mu=38959, 42115, 2346.5$  for *O*-CD, *M*-CD and *P*-CD, respectively. Our results confirm that the polarity of CDs in ground state is less than excited state ( $\mu_g < \mu_{ex}$ ). This study helps us understand the solvent-dependent behavior of nitrogen-doped carbon dots, particularly their solvent polarity characteristics. We also analyzed the optical properties of *M*-CD and found a linear response to the polarity and water content of the organic solvent, which suggests the possibility of *M*-CD as a humidity sensor for detecting water in organic solvents. *Prog. Color Colorants Coat. 18 (2025), 267-278* © Institute for Color Science and Technology.

### 1. Introduction

Fluorescent carbon nano dots (CDs) are gaining considerable attention as a novel quasi-organic-inorganic material. They possess properties like quantum dots, such as functionality and stability, while being superior due to the absence of environmental toxicity. These materials display organic dye-like behavior, which is

attributed to their noteworthy features such as excellent biocompatibility, pH stability, and water dispensability [1-4]. The distinctive characteristics of these materials render them highly desirable for a wide range of applications, including sensing [5-7], bio sensing [8, 9], semiconductors like as light-emitting diodes (LED) [10, 11], and solar cells components [12]. The CDs

\*Corresponding author: [\\*rouhani@icrc.ac.ir](mailto:*rouhani@icrc.ac.ir)

<https://doi.org/10.30509/pccc.2024.167381.1320>

luminescence is influenced by two main factors: the core or surface of CDs and the type of solvent. The emission spectra can be tuned by introducing functional groups and heteroatoms, like nitrogen, into CDs using reactants containing heteroatoms. Conjugated aromatic amines as nitrogen doping sources can affect the conjugated domain of CDs, changing the band gap and resulting in different photoluminescence properties [13, 14].

CDs are advanced systems that can be either 3D (spherical dot) or 2D (planar). In the case of planar CDs, the band gap is inversely proportional to the size of the  $\pi$ -conjugated  $sp^2$  carbon network, which is responsible for the  $\pi$  and  $\pi^*$  orbitals. To reduce the band gap, it is necessary to increase the conjugation with polyaromatic rings. Additionally, the presence of electron-donating groups with a non-bonding orbital ( $n$ ) located between the  $\pi$  and  $\pi^*$  orbitals can help to lower the band gap. As a result, decreasing the band gap leads to a redshift in the PL spectrum. The main sources of PL emission of CDs are from the hydrophobic  $sp^2$  carbon network ( $\pi$  to  $\pi^*$  transitions) in the core or at the surface and from heteroatom-based non-bonding orbitals ( $n$  to  $\pi^*$  transitions). The fluorophore surface is in contact with the solvent molecules and hence results in an interaction like H-bonding [15, 16]. Therefore, the sensitivity of CD emission to its surroundings makes it a good potential candidate for polar-sensitive probes. To date, numerous studies have been conducted to find ways to control the luminescence of CDs to design efficient sensors. However, the mechanism of emissive CDs is still not clearly verified. Therefore, deeper studies on the factors affecting the emission of fluorescent carbon dots are crucial in advancing the goal. We have synthesized CDs using a combination of citric acid and o,m,p-phenylenediamine as different nitrogen sources through the solvothermal method. The spectral characterization of CDs was studied in different solvents of varying polarities and in binary mixture solvents. The involved mechanisms were reported. We have also explored the possibility of humidity sensing of synthesized CDs.

## 2. Experimental

### 2.1. Material

The synthesis of O, P, and M-CD was done by our team based on literature [17]. Phenylenediamine derivatives, citric acid. All solvents utilized in the experiment were of analytical grade, indicative of their high purity and low impurity levels.

### 2.2. Apparatus

FTIR spectra were obtained via a SPECTRUM ONE spectrometer, providing functional group data. The photoluminescent properties were conducted using fluorescence spectroscopy (PerkinElmer). The morphological features were studied through SEM (Scanning Electron Microscopy (Tescan Mira3 LMU). Zeta Sizer (HORIBA SZ-100) was used to obtain the size of carbon dots.

### 2.3. Synthesis of carbon nano dots

Solvothermal method was used for preparation of carbon dots. Citric Acid (CA) and phenylene diamine derivatives were chosen as carbon and nitrogen sources, and dimethylformamide (DMF) as the solvent. This was based on previous studies [17]. To prepare the precursor, a solution of 1.68 g citric acid and 40 ml DMF was mixed with 0.64 g of each orthophenylenediamine (o-PDA), metaphenylenediamine (m-PDA), and paraphenylenediamine (p-PDA). The initial mixture was carefully prepared and stirred with precision to guarantee complete homogeneity. Once the mixture was ready, it was transferred to a specialized stainless-steel autoclave (with Teflon jacket), designed to withstand high pressure and temperature. The sealed autoclave was then placed in an oven, and heated at a precise temperature of 200 °C for a duration of 8 hours. This controlled heating process resulted in the formation of carbon nano dots. After the completion of reaction, cooling was done to room temperature. The resulting solution was heated at 80 °C to remove the solvent. The dry powder dissolved in dichloromethane. Then, slowly add DI water to the mixture while stirring it well until thoroughly combined. By centrifuging the solution for 10 minutes at 9000 rpm, resulting in the separation of two phases. The aqueous phase containing carbon dots were dried and used in the further process.

## 3. Results and Discussion

Three different conjugated nitrogen sources were selected based on phenylene diamine derivatives to study the photophysical characterization of CDs and their interactions with solvents. The nitrogen sources, which included o-PDA, m-PDA, and p-PDA, were selected to offer a comparative study and a deeper understanding of the surface functionality. The O-, M-, and P- CDs were synthesized and characterized using

several techniques. Firstly, the CDs were characterized by FTIR to distinguish the vibrational characteristic peaks of functional groups. The results showed that the M-CDs had plenty of hydrophilic groups on their surfaces, such as O–H and N–H ( $3200, 3358\text{ cm}^{-1}$ ), C–O–C/C–OH ( $1308\text{ cm}^{-1}$ ), and C=O ( $1708\text{ cm}^{-1}$ ) groups. These groups resulted in excellent solubility and stability of the M-CDs in water, which is important for their application. Figure 1 typically shows the vibrational characteristic peaks of functional groups on the M-CDs.

The Scanning Electron Microscopy (SEM) technique is used to examine the morphology of the synthesized CDs under solvothermal conditions (Figure 2A). The results indicate a uniform morphology of the CDs. Additionally, the EDX analysis in Figure 2B confirms the presence of nitrogen in the CDs as expected. The Zeta sizer result shows that the diameter of CDs is 3.2

nm (Figure 3). These results are consistent with the references and demonstrate well-synthesized carbon nano dots [18, 19].

### 3.1. Photophysical and solvatochromic properties

The concentration of carbon dots in aqueous solutions affects their luminescence. When the concentration of M-CDs increases, the emission intensity also increases significantly. This is because of the increased number of CDs in the solution, which results in higher density of emissive centers. However, at higher concentrations, the intensity may decrease due to C-dot aggregation and self-absorption, causing self-quenching effects (as shown in Figure 4). The critical concentration is 0.75 %, as illustrated in Figure 4. Conversely, at lower m-PD C-dot concentrations, the PL intensity is relatively weaker because of the limited number of CDs available to emit fluorescence.

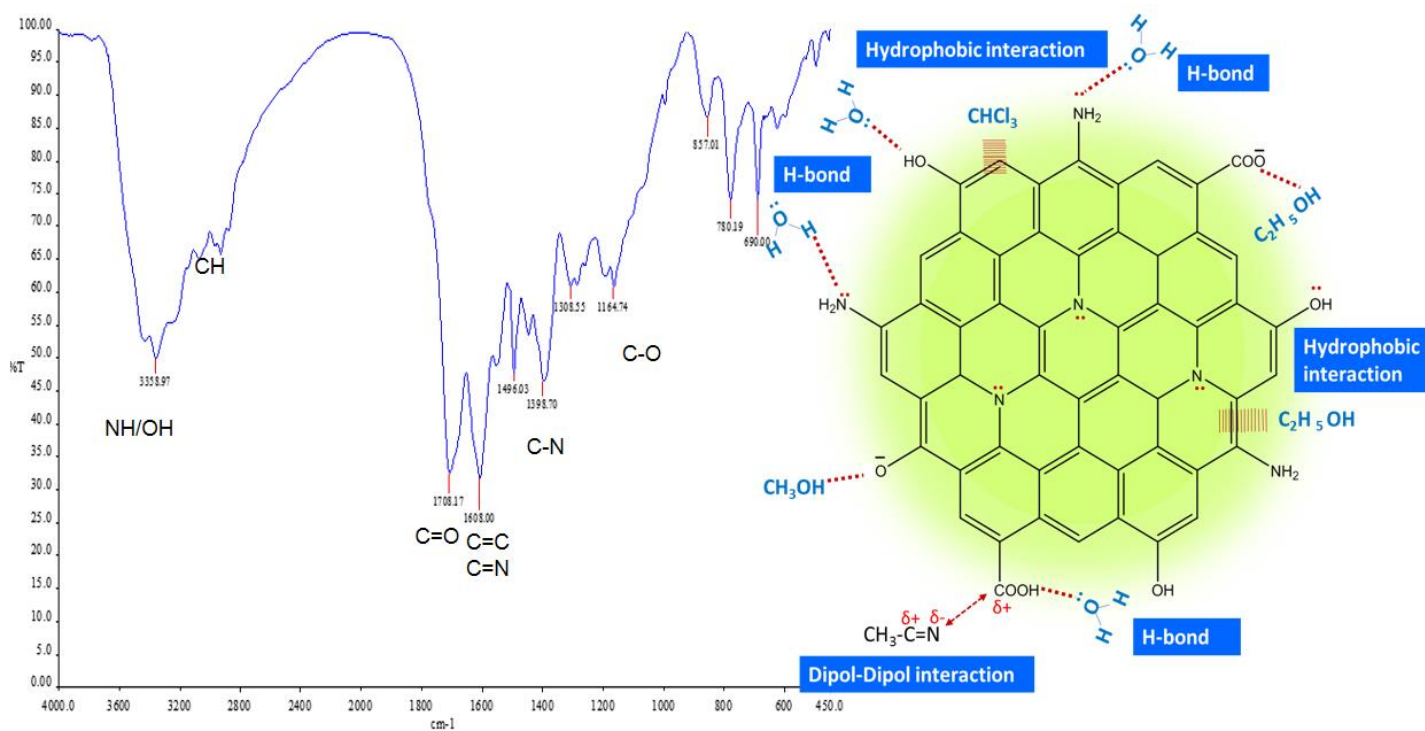


Figure 1: FT-IR spectra of M-CDs.

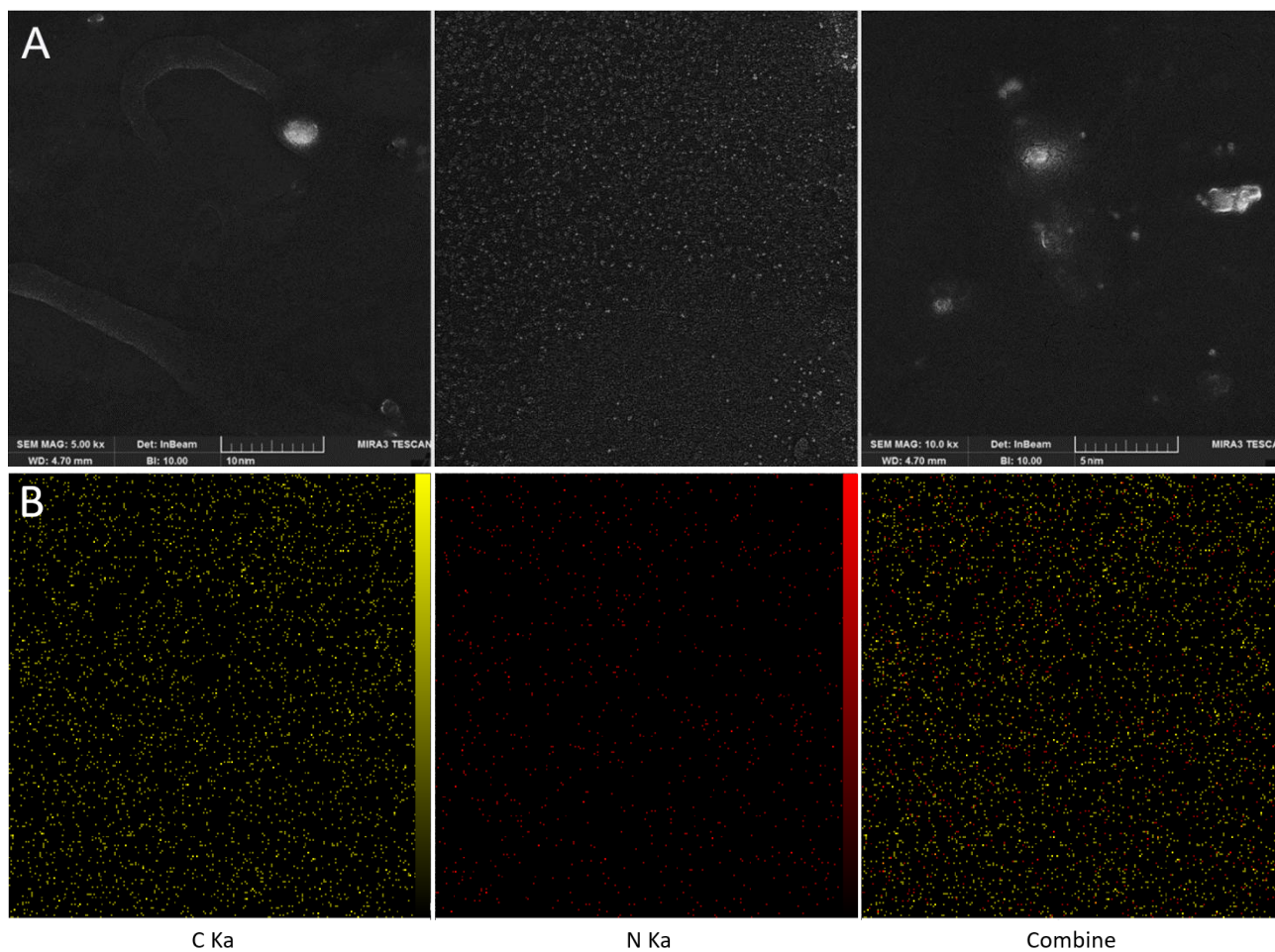


Figure 2: A) FE-SEM and B) EDX Map of M-CDs.

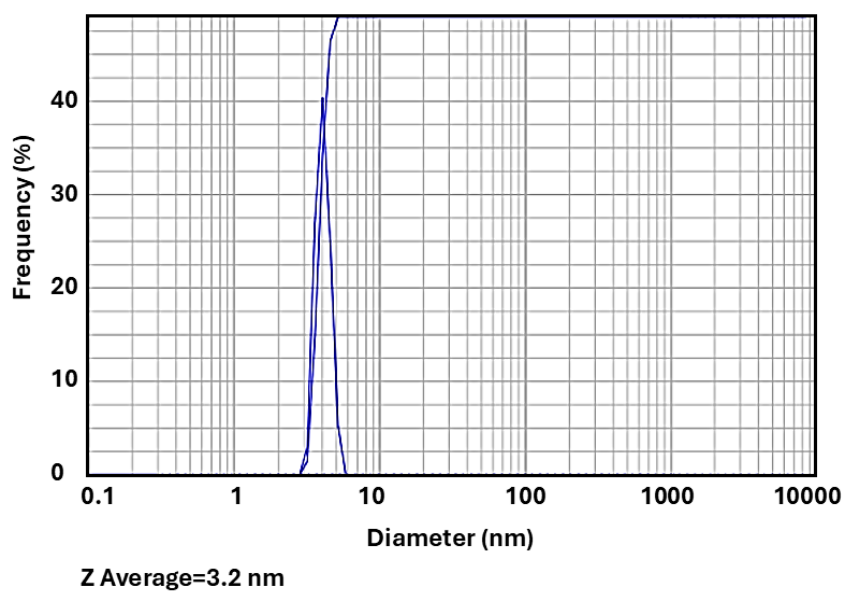
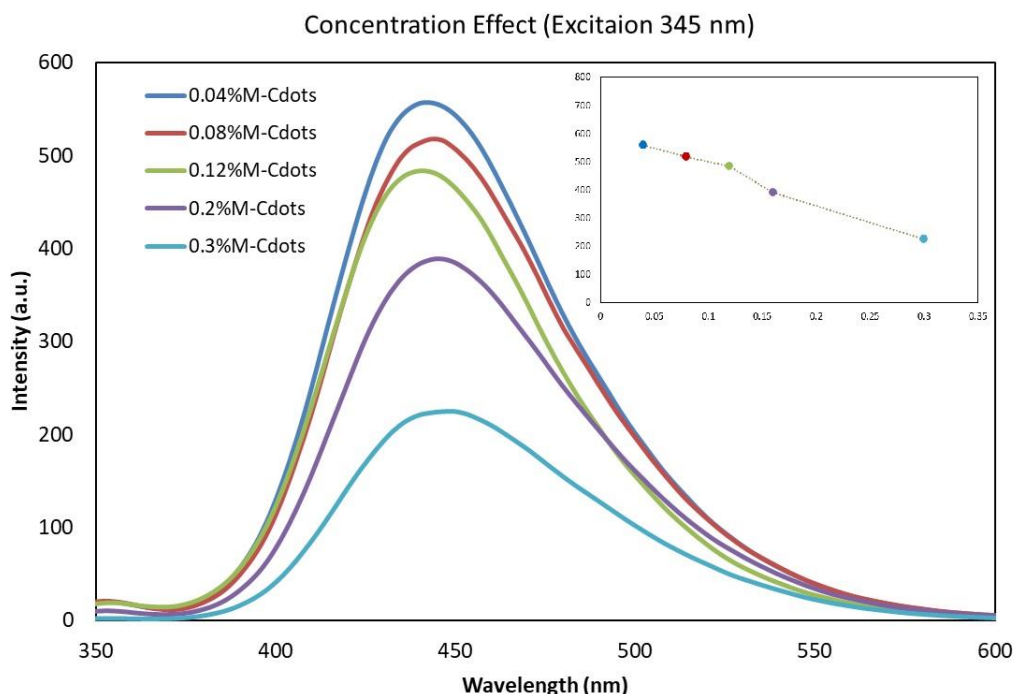


Figure 3: Zeta sizer results for M-CDs.



**Figure 4:** Dependency of PL intensity of M-CDs to the concentration of CDs in aqua solution.

### 3.2. pH Effect

Figure 5 displays the sensitivity of M-CDs to pH variations ranging from 1 to 13. Carbon dots are tiny particles that have a surface full of functional groups, including amino ( $\text{NH}_2$ ), carboxyl ( $\text{COOH}$ ), and hydroxyl ( $\text{OH}$ ) groups. Depending on the pH level, these groups can exist in various protonation or deprotonation states. The molecules' emission is determined by how they lose energy, either through the radiation path or non-radiative ways like interaction with the solvent, hydrogen bonding, and energy transfer to the solvent. Hence, changing the pH of the environment and surface charge can alter the non-radiative paths and result in a pH-dependent emission, which can be useful in designing a pH sensor [20, 21]. However, herein within the range of 6 to 11, the emission remains relatively stable.

### 3.3. Solvent effect

CDs, or carbon dots, demonstrate photophysical properties that are highly dependent on their surface groups such as hydroxyl, nitrogen and carboxylic acids. These amino-substituted groups possess nonbonding electrons, which have the ability to create a hydrogen bond or interact with the surrounding solvent, leading

to a change in spectral behavior. This polarization is solely responsible for their optical characteristics [22-24]. In Figure 6, the fluorescence and absorption spectra of CDs in  $\text{H}_2\text{O}$  are displayed, showcasing blue and yellow-green colors. The wavelength band around 300 nm confirms a charge transfer (CT) band, which observe for all CDs, due to the ( $\pi \rightarrow \pi^*$ ) transition [24]. The M-CD emission bands exhibited a significant 150 nm stock shift with a maximum ( $\lambda_{\text{em}} = 480 \text{ nm}$ ) shifted to the visible region. For P-CD, the wavelength band around 280 nm was shifted to the longer wavelengths ( $\lambda_{\text{em}} = 470 \text{ nm}$ ), showing a significant 190 nm stock shift. The emission band of O-CD moved to the visible region ( $\lambda_{\text{em}} = 523 \text{ nm}$ ), featuring a significant 260 nm stock shift. The stock shifts of these three isomers in water are completely different from each other, confirming that the carbon dots created differ in surface properties. They shift as follows: o-CD > p-CD > m-CD. To conduct a more detailed study, we analyzed the behavior of all three carbon dots in a group of solvents with varying polarities, which is illustrated in Figure 7. Table 1 summarizes the spectral data for synthesized CDs, and the solvents listed in order of their increasing polarity.



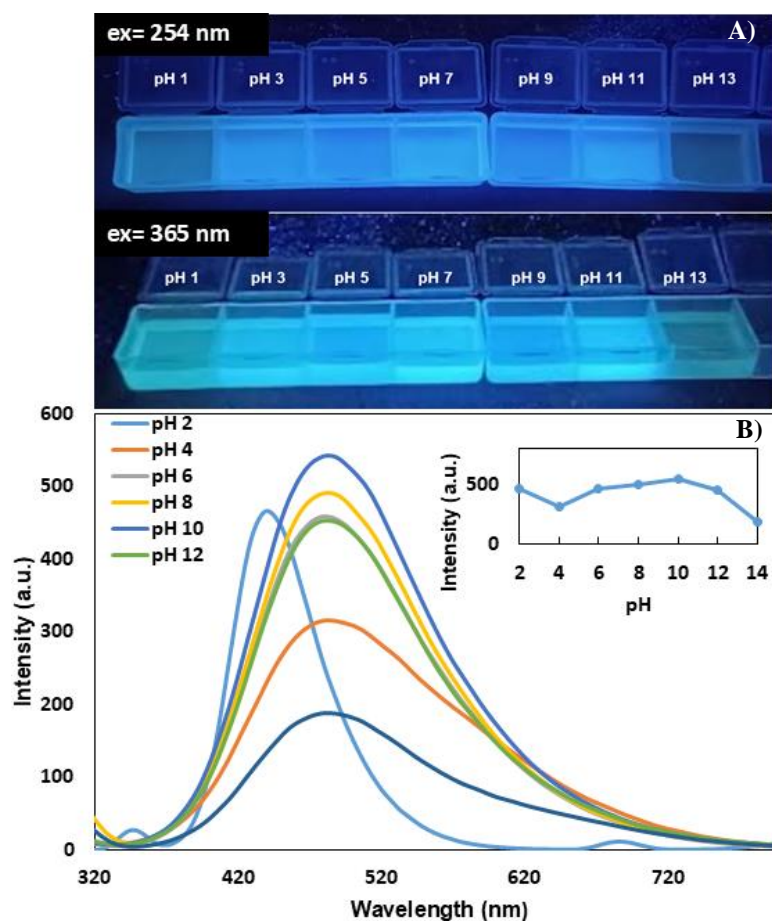


**Figure 5:** A) Photograph of aqueous M-CDs solution (0.04%) under UV light (254 and 366 nm) at pH 2-12; B) Emission spectra ( $\lambda_{\text{ex}}=340$  nm) aqueous solution of M-CDs. Inset. emission at maximum intensity vs. pH).

**Table 1:** Optical properties of CDs in different solvents.

Solvents	Solvent polarity index	$\Delta f$ ( $\text{cm}^{-1}$ )	O-CD				M-CD				P-CD			
			$\lambda_{\text{max}}^{\text{abs}}$ (nm)	$\lambda_{\text{max}}^{\text{em}}$ (nm)	FWHM ( $\text{cm}^{-1}$ )	$\nu_A - \nu_F$ ( $\text{cm}^{-1}$ )	$\lambda_{\text{max}}^{\text{abs}}$ (nm)	$\lambda_{\text{max}}^{\text{em}}$ (nm)	FWHM ( $\text{cm}^{-1}$ )	$\nu_A - \nu_F$ ( $\text{cm}^{-1}$ )	$\lambda_{\text{max}}^{\text{abs}}$ (nm)	$\lambda_{\text{max}}^{\text{em}}$ (nm)	FWHM ( $\text{cm}^{-1}$ )	$\nu_A - \nu_F$ ( $\text{cm}^{-1}$ )
PrOH	4	0.2716	234	497	68966	22614	355	614	59880	11882	390	478	104167	4721
$\text{CHCl}_3$	4.2	0.1502	257.5	400	86957	13835	353	548	52632	10080	392	486	121951	4934
Aceton	5.1	0.2841	328	522	91743	11331	355	583	53763	11016	389	478	90090	4786
MeOH	5.1	0.3080	258	617	50000	22552	274.5	590	48077	19481	360	482	133333	7031
EtOH	5.2	0.2887	256	498	94340	18982	354.5	621	68493	12106	387	490	99010	5432
DMF	6.4	0.2742	269.5	525	90090	18058	358	600	51813	11266	391	528	78740	6636
$\text{H}_2\text{O}$	10.2	0.3199	259.5	600	38168	21869	295.5	590	56818	16892	388.5	460	112360	4001

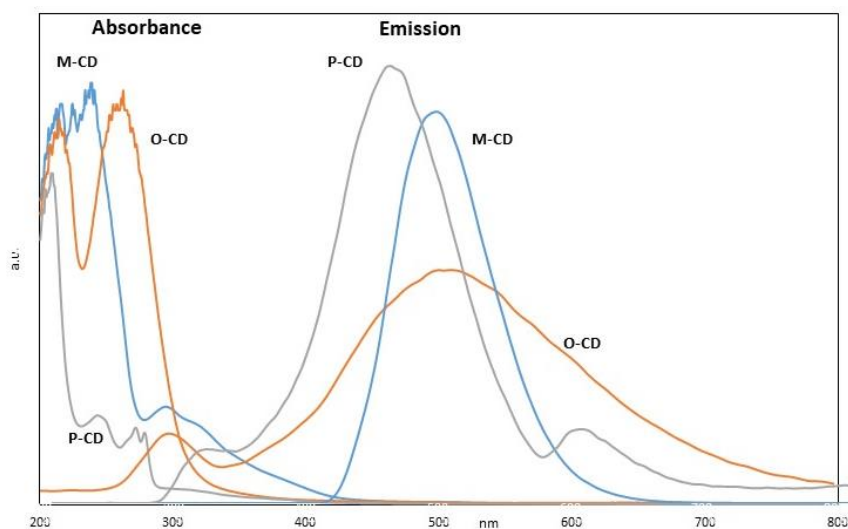


Figure 6: Absorption and emission spectra of CDs in H<sub>2</sub>O.

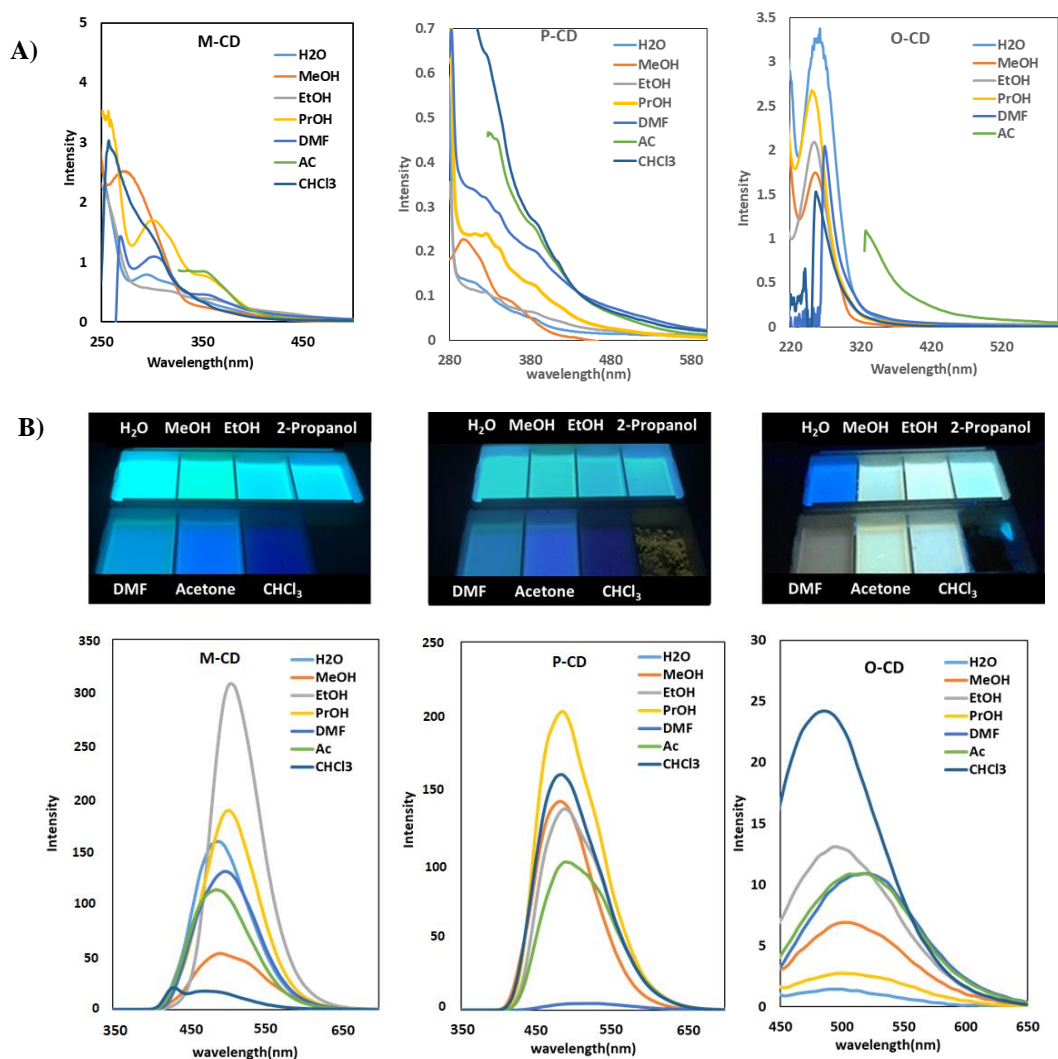
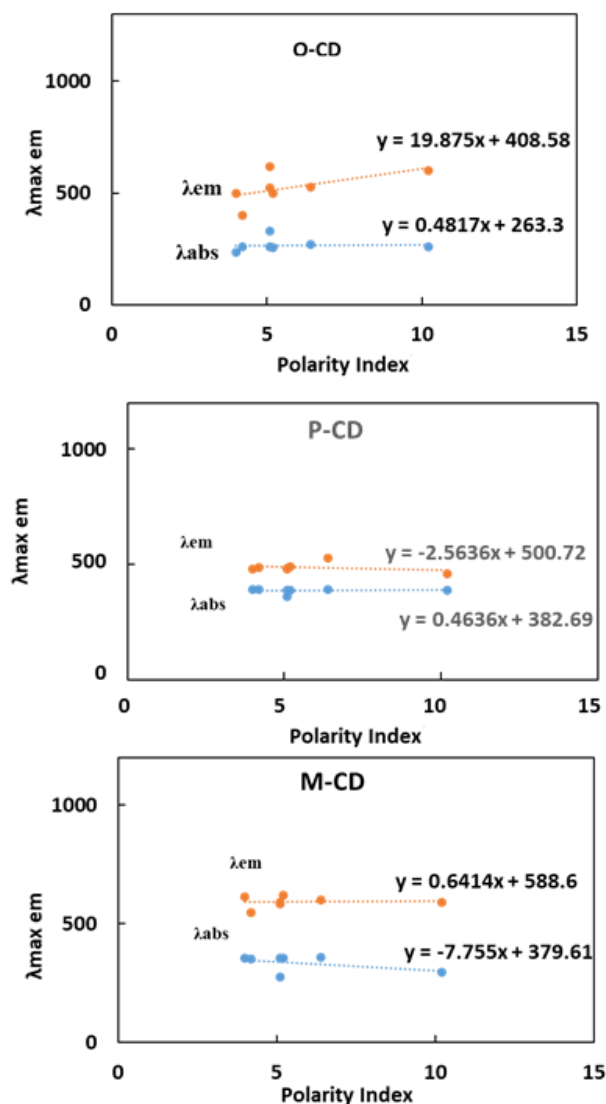


Figure 7: A) Absorption and B) emission spectra of CDs in different solvents. Photograph of dispersed CDs in various solvents under (366 nm) UV light.

Scientific studies have shown that the degree of polarity in an environment has a minimal impact on the absorption spectrum [24]. In Figures 7A and 7B, it is evident that there are only a few instances of redshifts observed in the absorption and emission bands of P-CD. This finding indicates that P-CD is relatively insensitive to changes in the environment's polarity, making it a stable and reliable option for various applications. The absorption maxima changed from 360 nm in MeOH to 392 in  $\text{CHCl}_3$ , while the emission band shifted 68nm and the absorbance shifted 32 nm. It is noted that O-CD and M-CD show different changes in the absorbance and emission bands. For M-CD, the absorption maxima occur between 295-355 nm in  $\text{H}_2\text{O}$ -DMF (60 nm), while the emission maxima change between 548-621 nm (73 nm) (Table 1). In order to conduct a thorough analysis of the impact of solvents on spectral shift, it is imperative to carefully compare the stock shifts mentioned in Table 1. The plot in Figure 8 clearly shows that the slope of the absorption and emission spectra against solvent polarity reflects the dependency of sensitivity to solvent polarity. The slope of the linear line emission is more sensitive than absorption, indicating that the sensitivity of emission with respect to polarity follows the order O-CD > M-CD > P-CD. It is important to note that the solvent polarity shows less effect on absorption spectra, due to the the same local environment in both the ground and excited state of molecules. Light absorption occurs rapidly, in a timeframe of approximately  $10^{-15}$  seconds, which is too short for the fluorophore's movement. When a fluorophore emits light, it is surrounded by solvent molecules that are arranged in a specific orientation around the excited state. This arrangement makes the fluorophore highly sensitive to the polarity of the surrounding solvent. As a result, changes in solvent polarity can greatly affect the way the fluorophore emits light. However, the emitting polar excited molecules cause the orientation of solvent molecules around them, which makes it far more sensitive to solvent polarity [24]. This phenomenon can have a significant impact on the interpretation of spectroscopic data and should be taken into account when analyzing experimental results.

The absorption and emission of molecules are affected by the solvents they are in. This is due to the dipole moments of these molecules being more significant in their excited state than in their ground state. This phenomenon is known as a "charge-transfer

transition" or solvent relaxation. However, this process requires significant solvent reorganization energies, which can increase nonradiative decay rate [23]. The results of the study demonstrate that M-CD and O-CD have a positive slope, while P-CD has a near-constant or negative slope. Another parameter for deeper study of solvent effect is the full width at half maximum (FWHM). Results in Figure 9 show, by increasing solvent polarity, the CD FWHM decreases. Although there is no clear correlation in the data presented in Table 1.



**Figure 8:** Absorption and emission of CDs at maximum wavelength vs solvent polarity.



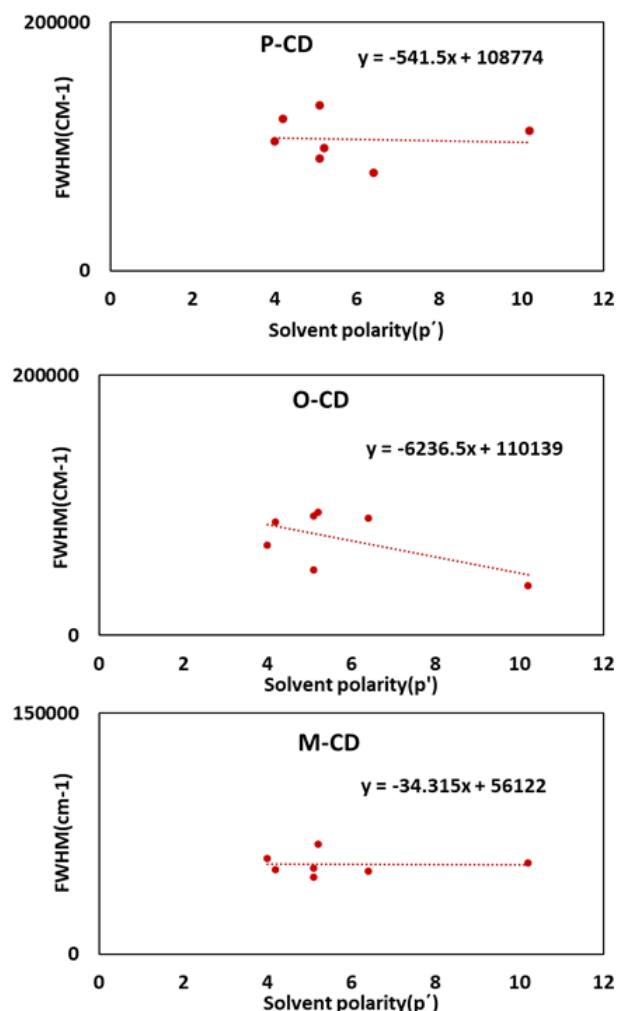


Figure 9: FWHM changes of CD with solvent polarity.

The researchers in this study selected a set of solvents with varying polarities to obtain a comprehensive understanding of how they affect a given system. Their findings suggest that modifications in spectral responses due to solvent polarity can be accurately expressed by dipole moments of both the ground and excited states. The researchers further discovered that fluorophores with greater dipole moment alterations display a heightened sensitivity to solvent polarity. This intriguing phenomenon is approximated using a Lippert-Mataga plot (equation 1) [25, 26], which is essentially a graphical representation of Stokes shift versus solvent polarity. It is worth noting that the symbol  $\Delta\nu$  represents the difference between the maximum absorption and emission wavelengths.

$$\nu_A - \nu_F = \frac{2}{hc} \left( \frac{\varepsilon-1}{2\varepsilon+1} - \frac{n^2-1}{2n^2+1} \right) \frac{(\mu_e - \mu_g)^2}{a^3} \quad (1)$$

The equation presented here describes the difference between the dipole moments of the excited and ground states of a fluorophore, denoted as  $\Delta\mu$ . This difference is influenced by several constants, including Planck's constant ( $h$ ), the speed of light ( $c$ ), and the radius of the Onsager cavity around the fluorophore ( $a$ ). Additionally, the solvent's dielectric constant ( $\varepsilon$ ) and refractive index ( $n$ ) play a role in this equation. The quantity " $\Delta f$ " in equation 2 represents the solvent's orientation polarizability, which refers to how easily the solvent molecules can align with an external electric field. To examine this concept further, researchers often refer to the Lippert-Mataga plot, which depicts changing the fluorophore's Stokes shift with the solvent's orientational polarizability. Figure 10 shows the Lippert-Mataga plot specifically for CDs, demonstrating a clear positive linear correlation between CDs' Stokes shift and increasing polarity. The slope of this dependence for O-CD, M-CD and P-CD is  $\Delta\mu = 38959, 42115, 2346.5$  respectively, which follow the order of M-CD > O-CD >> P-CD. Results of Figure 8 and Lippert-Mataga plot show the P-CD is less sensitive to polarity, which confirms different surface characteristics of isomeric CDs used.

$$\Delta f = \frac{\varepsilon-1}{2\varepsilon+1} - \frac{n^2-1}{2n^2+1} \quad (2)$$

The data presented in Figure 10 provides clear evidence that an increase in polarity of solvent results in a significant increase in energy. The positive slope of the graph indicates that the compounds being studied have a higher polarity character in their excited state than in ground state ( $\mu_g < \mu_{ex}$ ). Additionally, a small solvent effect observed in the ground state, which causes a higher degree of solvent reorientation around the excited state. Interestingly, the results also show that P-CD is less sensitive, implying that the polarity of the ground and excited state of this molecule is similar. These findings shed new light on the behavior of these compounds under varying solvent conditions and provide valuable insights for future research in this area.

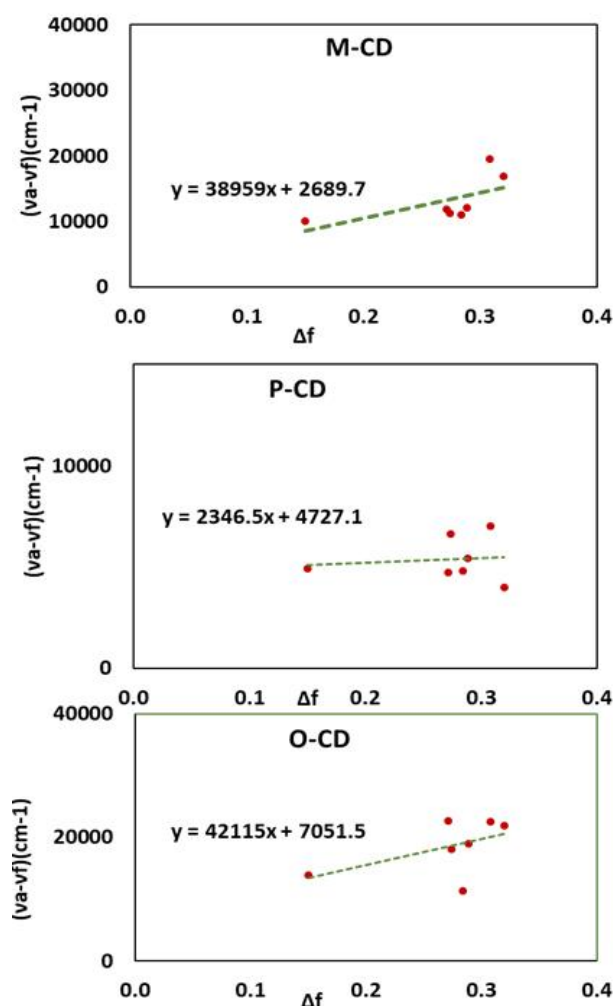
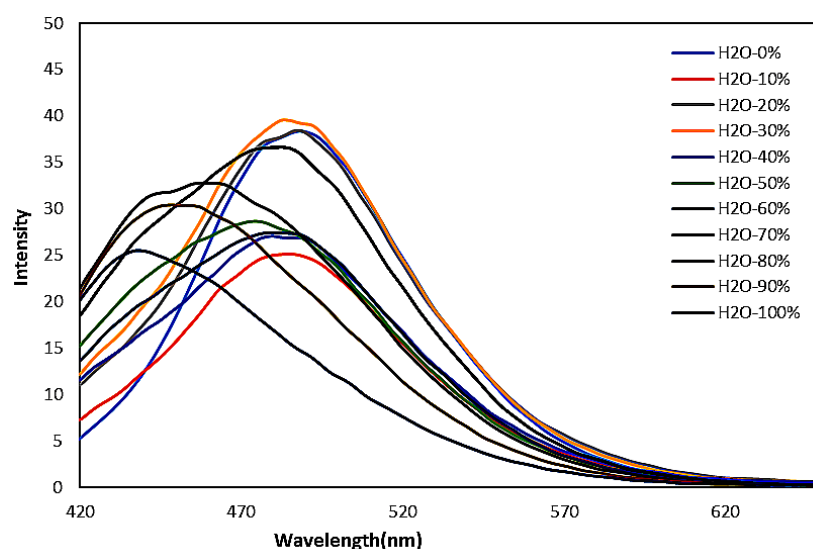


**Figure 10:** Plot of the Stokes shifts of CD vs. solvent's orientation polarizability ( $\Delta f$ ).

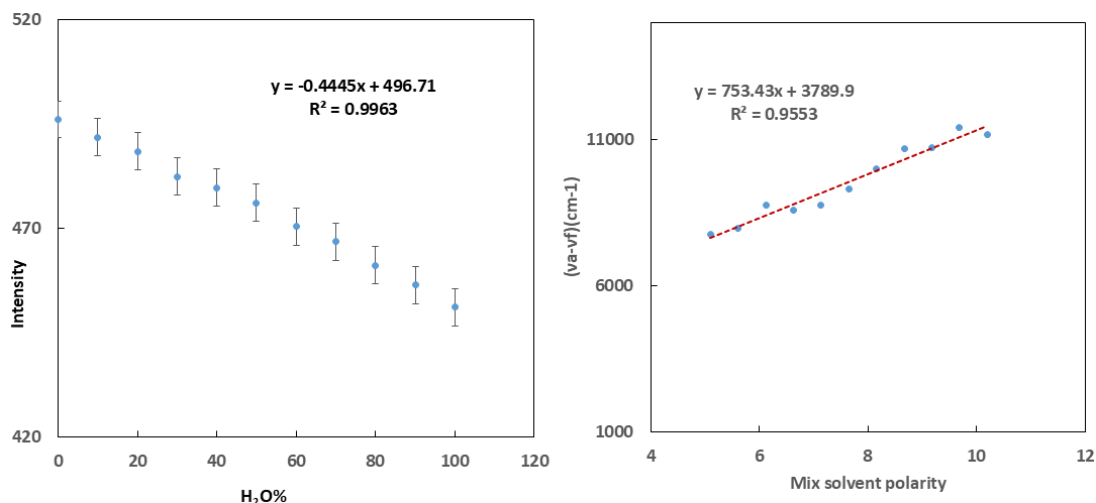
Polarity sensitivity results suggest that O-CD and M-CD can be useful candidates for polarity sensing and applied as humidity sensors. M-CD was chosen to study the sensing behavior of CDs against  $\text{H}_2\text{O}$ . A binary mixture of  $\text{H}_2\text{O}$ -Acetone and  $\text{H}_2\text{O}$ -DMF with varying percentages of  $\text{H}_2\text{O}$  was prepared, and the absorbance and emission of M-CD in the  $\text{H}_2\text{O}$ -Acetone binary mixture were recorded (Figure 11). As the percentage of  $\text{H}_2\text{O}$  increases, the polarity of the mixture also increases, leading to a shift in the maximum emission of M-CD towards longer wavelengths. Figure 12 shows the stock shift versus  $\text{H}_2\text{O}$  % and solvent polarity, indicating a good linear relationship between  $\text{H}_2\text{O}$  %, solvent polarity, and stock shift. These can be used as calibration curves.

Figure 12 presents the linear relationship between intensity and medium polarity and water content, indicating that it is suitable for detecting polarity. The sensitivity of a sensor can be determined by examining the slope of the calibration curve for the linear regression line, as well as the standard deviation of the emission peak. These values can then be used to calculate the detection limit using the following formula: S/N ratio of 3. The standard deviation of response ( $S_a$ ) and the sensitivity of the calibration curve ( $b$ ) are represented by the equation below, which shows the detection limit of the sensor for determining water content in acetone.

$$\text{LOD (Limit of Detection)} = 3S_a/b$$



**Figure 11:** Emission of M-CD in binary mixture  $\text{H}_2\text{O}$ -Acetone.



**Figure 12:** Emission at maximum wavelength of M-D at maximum wavelength vs (left) % H<sub>2</sub>O and (right) mix solvent polarity H<sub>2</sub>O-Acetone.

The LOD of water detection in ethanol was calculated by plotting emission at the maximum wavelength versus H<sub>2</sub>O%, with 0.59 Sa obtained at 3.9% for three measurements (n=3). These results suggest that the developed CDs in this study are good candidate for detection of the water content in organic solvents.

#### 4. Conclusion

The synthesis of nitrogen-doped carbon dots was successfully achieved by utilizing three isomers of phenylenediamine (o-PDA, m-PDA, and p-PDA) as nitrogen sources and citric acid as the carbon source. The optical properties of carbon dots are heavily influenced by the solvent used. The fluorescence emission of the carbon dots was studied in a range of

solvents, from weakly polar CHCl<sub>3</sub> to strongly polar protic water and a binary mixture of H<sub>2</sub>O-Acetone. The results showed that as solvent polarity increased, the emission band shifted to longer wavelengths. The Lippert-Mataga plot revealed that all CDs had a positive linear dependence on increasing polarity, conclusively demonstrating that the CDs have a more polarity in the excited state respect to the ground state ( $\mu_g < \mu_{ex}$ ). Among these derivatives, P-CD was found to be less sensitive. The polarity sensitivity results suggest that O-CD and M-CD are promising candidates for polarity sensing and can be applied as humidity sensors. Furthermore, upon analyzing the optical properties of M-CD, against to the solvent polarity and water content of the organic solvent, making it an ideal choice for detecting polarity.

#### 5. References

- Koutsogiannis P, Thomou E, Stamatis H, Gournis D, Rudolf P. Advances in fluorescent carbon dots for biomedical applications. *Adv Phys X*. 2020;5(1): 1758592. <https://doi.org/10.1080/23746149.2020.1758592>.
- Li X, Zhao S, Li B, Yang K, Lan M, Zeng L. Advances and perspectives in carbon dot-based fluorescent probes: Mechanism, and application. *Coordin Chem Rev*. 2021;431:213686. <https://doi.org/10.1016/j.ccr.2020.213686>.
- Jorns M, Pappas D. A review of fluorescent carbon dots, their synthesis, physical and chemical characteristics, and applications. *Nanomaterials*. 2021; 11(6):1448. <https://doi.org/10.3390/nano11061448>.
- Zuo J, Jiang T, Zhao X, Xiong X, Xiao S, Zhu Z. Preparation and application of fluorescent carbon dots. *J Nanomater*. 2015; 2015:10-.
- Sun X, Lei Y. Fluorescent carbon dots and their sensing applications. *TrAC Trends Anal Chem*. 2017; 89:163-80. <https://doi.org/10.1155/2015/787862>.
- Yoo D, Park Y, Cheon B, Park MH. Carbon dots as an effective fluorescent sensing platform for metal ion detection. *Nanoscale Res Lett*. 2019;14:1-3. <https://doi.org/10.1016/j.trac.2017.02.001>
- Alvandi N, Ranjbar Z, Esfandiari N. Fe (III) detection by multicolor carbon dots as fluorometric probes. *Prog Color Colorant Coat*. 2024; 17(1):11-25. <https://doi.org/10.30509/pccc.2023.167138.1218>.

8. Li H, Yan X, Kong D, Jin R, Sun C, Du D, Lin Y, Lu G. Recent advances in carbon dots for bioimaging applications. *Nanoscale Horizons*. 2020; 5(2):218-34. <https://doi.org/10.1039/C9NH00476A>.
9. Peng Z, Han X, Li S, Al-Youbi AO, Bashammakh AS, El-Shahawi MS, Leblanc RM. Carbon dots: biomacromolecule interaction, bioimaging and nanomedicine. *Coord Chem Rev*. 2017; 343:256-77. <https://doi.org/10.1016/j.ccr.2017.06.001>.
10. Zhao B, Tan ZA. Fluorescent carbon dots: fantastic electroluminescent materials for light-emitting diodes. *Adv Sci*. 2021; 8(7):2001977. <https://doi.org/10.1002/adv.202001977>.
11. Yuan F, Wang YK, Sharma G, Dong Y, Zheng X, Li P, Johnston A, Bappi G, Fan JZ, Kung H, Chen B. Bright high-colour-purity deep-blue carbon dot light-emitting diodes via efficient edge amination. *Nature Photonics*. 2020; 14(3):171-6. <https://doi.org/10.1038/s41566-019-0557-5>.
12. Wang H, Sun P, Cong S, Wu J, Gao L, Wang Y, Dai X, Yi Q, Zou G. Nitrogen-doped carbon dots for "green" quantum dot solar cells. *Nanoscale Res Lett*. 2016;11:1-6. <https://doi.org/10.1186/s11671-016-1231-1>.
13. Yuan YH, Liu ZX, Li RS, Zou HY, Lin M, Liu H, Huang CZ. Synthesis of nitrogen-doping carbon dots with different photoluminescence properties by controlling the surface states. *Nanoscale*. 2016; 8(12):6770-6. <https://doi.org/10.1039/C6NR00402D>.
14. Lin C, Zhuang Y, Li W, Zhou TL, Xie RJ. Blue, green, and red full-color ultralong afterglow in nitrogen-doped carbon dots. *Nanoscale*. 2019;11(14):6584-90. <https://doi.org/10.1039/C8NR09672D>.
15. Wei S, Yin X, Li H, Du X, Zhang L, Yang Q, Yang R. Multi-color fluorescent carbon dots: graphitized sp<sup>2</sup> conjugated domains and surface state energy level Co-modulate band gap rather than size effects. *Chem-A European J*. 2020; 26(36), 8129-8136. <https://doi.org/10.1002/chem.202000763>.
16. Yuan YH, Liu ZX, Li RS, Zou HY, Lin M, Liu H, Huang CZ. Synthesis of nitrogen-doping carbon dots with different photoluminescence properties by controlling the surface states. *Nanoscale*. 2016; 8(12):6770-6. <https://doi.org/10.1039/C6NR00402D>.
17. Jiang K, Sun S, Zhang L, Lu Y, Wu A, Cai C, Lin H. Red, green, and blue luminescence by carbon dots: full-color emission tuning and multicolor cellular imaging. *Angewandte chemie*. 2015; 127(18):5450-3. <https://doi.org/10.1002/ange.201501193>.
18. Ji C, Han Q, Zhou Y, Wu J, Shi W, Gao L, Leblanc RM, Peng Z. Phenylenediamine-derived near infrared carbon dots: The kilogram-scale preparation, formation process, photoluminescence tuning mechanism and application as red phosphors. *Carbon*. 2022; 192:198-208. <https://doi.org/10.1016/j.carbon.2022.02.054>.
19. Ye Y, Yang D, Chen H, Guo S, Yang Q, Chen L, Zhao H, Wang L. A high-efficiency corrosion inhibitor of N-doped citric acid-based carbon dots for mild steel in hydrochloric acid environment. *Journal of hazardous materials*. 2020; 381:121019. <https://doi.org/10.1016/j.jhazmat.2019.121019>.
20. Dutta Choudhury S, Chethodil JM, Gharat PM, PK P, Pal H. pH-elicited luminescence functionalities of carbon dots: mechanistic insights. *J Phys Chem Lett*. 2017;8(7):1389-95. <https://doi.org/10.1021/acs.jpcclett.7b00153>.
21. Sui L, Jin W, Li S, Liu D, Jiang Y, Chen A, Liu H, Shi Y, Ding D, Jin M. Ultrafast carrier dynamics of carbon nanodots in different pH environments. *Phys Chem Chem Phys*. 2016; 18(5):3838-45. <https://doi.org/10.1039/C5CP07558K>.
22. Zhang T, Zhu J, Zhai Y, Wang H, Bai X, Dong B, Wang H, Song H. A novel mechanism for red emission carbon dots: hydrogen bond dominated molecular states emission. *Nanoscale*. 2017; 9(35):13042-51. <https://doi.org/10.1039/C7NR03570E>.
23. Papaioannou N, Marinovic A, Yoshizawa N, Goode AE, Fay M, Khlobystov A, Titirici MM, Sapelkin A. Structure and solvents effects on the optical properties of sugar-derived carbon nanodots. *Sci Report*. 2018; 8(1):6559. <https://doi.org/10.1038/s41598-018-25012-8>.
24. Chao D, Lyu W, Liu Y, Zhou L, Zhang Q, Deng R, Zhang H. Solvent-dependent carbon dots and their applications in the detection of water in organic solvents. *J Mater Chem C*. 2018; 6(28):7527-32. <https://doi.org/10.1039/C8TC02184H>.
25. Bozkurt E, Gul HI, Mete E. Solvent and substituent effect on the photophysical properties of pyrazoline derivatives: A spectroscopic study. *J Photochem Photobiol A: Chem*. 2018; 352:35-42. <https://doi.org/10.1016/j.jphotochem.2017.10.010>.
26. Mahdiani M, Rouhani S, Zahedi P. Synthesis, Solvatochromism and fluorescence quenching studies of naphthalene diimide dye by nano graphene oxide. *J Fluorescence*. 2023; 1-2. <https://doi.org/10.21203/rs.3.rs-2428740/v1>.

How to cite this article:

Kaviani Darani M, Rouhani Sh, Ranjbar Z. Deep Fluorescence Solvatochromic Study of Nitrogen Doped Carbon Dots: Polar Sensitive Nanoprobe Application. *Prog Color Colorants Coat*. 2025;18(3):267-278. <https://doi.org/10.30509/pccc.2024.167381.1320>.

